IOP Publishing New J. Phys. 27 (2025) 023027 https://doi.org/10.1088/1367-2630/adb174

New Journal of Physics
The open access journal at the forefront of physics

Deutsche Physikalische Gesellschaft DPG
IOP Institute of Physics

Published in partnership with: Deutsche Physikalische Gesellschaft and the Institute of Physics

OPEN ACCESS

RECEIVED
15 October 2024

REVISED
21 January 2025

ACCEPTED FOR PUBLICATION
3 February 2025

PUBLISHED
21 February 2025



PAPER

# Unlocking the advantage of qubit communication in multi-node network configurations

**Ananya Chakraborty[1], Sahil Gopalkrishna Naik[1], Edwin Peter Lobo[2], Ram Krishna Patra[1], Samrat Sen[1], Mir Alimuddin[3], Amit Mukherjee[4,*] and Manik Banik[1]**

[1] Department of Physics of Complex Systems, S. N. Bose National Center for Basic Sciences, Block JD, Sector III, Salt Lake, Kolkata 700106, India
[2] Laboratoire d'Information Quantique, Universite libre de Bruxelles (ULB), Av. F. D. Roosevelt 50, 1050 Bruxelles, Belgium
[3] ICFO-Institut de Ciencies Fotoniques, The Barcelona Institute of Science and Technology, Av. Carl Friedrich Gauss 3, 08860 Castelldefels (Barcelona), Spain
[4] Indian Institute of Technology Jodhpur, Jodhpur 342030, India
* Author to whom any correspondence should be addressed.

**E-mail:** amitm.qm@gmail.com

**Keywords:** qubit communication, multiple access channel, quantum advantage, quantum entanglement, quantum nonlocality without entanglement

## Abstract

The extension of point-to-point communication to multi-node configurations has significant applications in internet and telecommunication networks. Quantum resources promise notable advantages in such settings. Here, we demonstrate a novel quantum advantage in simulating multiple access channels (MACs)-a common network configuration where multiple distant senders transmit messages to a single receiver (e.g. the uplink from several mobile phones to a server). Specifically, we show that qubit transmission outperforms its classical counterpart, even when the latter is supplemented with classical shared randomness. Remarkably, unlike the seminal quantum superdense coding protocol, this advantage is achieved without any pre-shared entanglement between the senders and the receiver-a feat prohibited by Holevo and Frenkel–Weiner no-go theorems in the one-sender-one-receiver scenario. The receiver's ability to simultaneously decode quantum systems from multiple senders underpins this distinct advantage in the MAC setup. Some of our MAC designs are inspired by constructs in quantum foundations, such as the Pusey–Barrett–Rudolph theorem and 'quantum nonlocality without entanglement'. Beyond network applications, this quantum advantage reveals a deeper connection to 'quantum nonlocality without inputs' phenomenon and suggests potential for semi-device-independent certification of entangled measurements.

## 1. Introduction

The elementary model of communication, originally formulated in Claude Shannon's seminal 1948 work [1], addresses the reliable transmission of information between two distant servers. Its quantum counterpart-quantum Shannon theory [2]-seeks to exploit the non-classical properties of quantum systems to enhance information transmission rates [3]. For instance, the celebrated quantum superdense coding protocol leverages quantum entanglement, pre-shared between a sender and a receiver, to transmit two bits of classical information by communicating a two-level quantum system [4]. Subsequently, this study was extended to noisy quantum channels, leading to the concept of entanglement-assisted classical capacity of a quantum channel [5–7]. However, quantum advantages come with inherent limitations, such as the Holevo's theorem, which constrains the communication capacity of a quantum system to be the same as its classical counterpart in the absence of any pre-shared entanglement [8]. More recently, Frenkel and Weiner extended this result, showing that any input–output correlation achievable with an $n$-level quantum system can also be achieved through an $n$-state classical system when no entanglement is pre-shared between the sender and receiver [9]. This, in turn, renders the 'signaling dimension' of quantum and classical systems identical,

further motivating the study of the structure of composite physical systems based on timelike correlations. [10] (see also [11–13]).

Here, we present a novel advantage of quantum communication in the network setting involving multiple distant parties exchanging information among themselves [14]. Specifically, we demonstrate that communicating a quantum system outperforms its classical counterpart in a widely used communication network called the multiple access channel (MAC) [15–18]. Crucially, unlike the superdense coding protocol, this advantage is achieved without any pre-shared entanglement between the senders and receivers. A MAC involves multiple distant senders transmitting their respective messages to a common receiver, such as the uplink signals from several mobile users on the ground to a common satellite server (see figure 1). In simulating a MAC, the goal is to replicate its function with minimal communication between the senders and the receiver. Remarkably, we identify instances where transmitting qubits from each sender enables MAC simulation tasks that become infeasible when qubit channels are replaced with classical bit (c-bit) channels. Moreover, this quantum advantage persists even when the classical channels are supplemented with unlimited classical correlations (also called shared randomness (SR)). Notably, some of our MAC designs draw inspiration from well-known results in quantum foundations. For instance, building on the Pusey–Barrett–Rudolph (PBR) theorem [19], which establishes that the quantum wavefunction represents the reality of a physical system rather than merely a description of it, we construct a two-sender MAC that demonstrates the desired quantum advantage. We then explore another intriguing concept, known as 'quantum nonlocality without entanglement' (QNWE) [20], where an orthogonal product basis of a composite quantum system cannot be perfectly discriminated using local operations and classical communication (LOCC). However, being mutually orthogonal, these states can be perfectly distinguished under global operations. Leveraging this concept we design a distinct three-sender MAC. We further propose a generic approach to construct a class of MACs, all demonstrating quantum advantages. Importantly, the origin of the quantum advantages crucially lies in the receiver's ability to jointly process the quantum systems received from multiple senders, enabling global decoding that surpasses the limitations imposed by the Holevo–Frenkel–Weiner no-go theorems in one-sender-one-receiver communication setups [8, 9].

## 2. Communication in network scenario

The simplest communication setup involves a sender and a receiver, with their shared goal reducing to the task of channel simulation. A channel connecting the sender $S$ and receiver $R$ is mathematically described as a stochastic map from the sender's input alphabet to the receiver's output alphabet. This is expressed by the probability vector $\mathcal{N} = \{p(a|x) \mid a \in A, x \in X\}$, where $X$ denotes the sender's input set, $A$ the receiver's output set, and $p(a|x)$ the probability of output $a \in A$ given input $x \in X$, satisfying $\sum_{a\in A} p(a|x) = 1$ for all $x \in X$. To simulate the channel, the sender encodes input $x$ into a physical state $\omega_x$, which is transmitted to the receiver via a channel described by the action $\Lambda : \Omega_{\text{in}} \to \Omega_{\text{out}}$, where $\Omega_{\text{in}}$ and $\Omega_{\text{out}}$ are the state spaces of input and output systems, respectively. The channel may distort the transmitted state, resulting in $\omega_y$ at the receiver instead of $\omega_x$. The receiver then performs an operation $\mathcal{O}$ on the received state, producing an output $a \in A$. In an ideal noiseless scenario, the task may require the receiver to infer the sender's input $x$. The information transfer is quantified by the mutual information $I(X : A)$, which measures the shared information between $X$ and $A$, i.e. $I(X : A) = H(X) - H(X|A)$, where $H(X)$ is the entropy of $X$, and $H(X|A)$ is the conditional entropy of $X$ given $A$, defined as $H(X|A) = H(X, A) - H(A)$. This quantifies the average uncertainty about $X$ given knowledge of $A$. When the sender uses a two-level classical system (a cbit) to encode $X$, the maximum mutual information the receiver can achieve is 1 bit. For its quantum counterpart, the qubit, infinite pure-state encodings are possible. However, the no-go theorem of Holevo establishes that even for qubits, the mutual information remains bounded by 1 bit. More recently a stricter version of this no-go result is established by Frenkel and Weiner [9]. They have demonstrated that the set of achievable probability distributions $\{p(a|x)\}$ using an $n$-level quantum system is identical to that achievable by an $n$-level classical system. Notably, this result assumes SR as a free resource. Subsequent studies, however, explored scenarios where SR is treated as a costly resource, leading to advantages of qubit communication over it classical counterpart [21–23].

An important question here concerns the status of Frenkel and Weiner kind of no-go result in network settings. We investigate a particular network scenario that involves multiple senders and a single receiver, commonly known as the MAC. Mathematically, a MAC is represented as a stochastic map from the input alphabets of the senders to the output alphabet of the receiver. A MAC with $K$ senders $\{S_i\}_{i=1}^K$ and one receiver $R$ is described by the probability vector $\mathcal{N}^K = \{p(a|x_1, \ldots, x_K) \mid a \in A, x_i \in X_i\}$, where $X_i$ is the input set of the $i$th sender, $A$ is the receiver's output set, and $p(a|x_1, \ldots, x_K)$ represents the probability of outcome $a \in A$ given inputs $x_i \in X_i$. This satisfies $\sum_{a\in A} p(a|x_1, \ldots, x_K) = 1$ for all $\vec{x} = (x_1, \ldots, x_K) \in \prod_{i=1}^K X_i$. We demonstrate that quantum communication offers significant advantages over classical communication in certain channel simulation tasks, even when the receiver shares independent unlimited classical correlations

with each sender. Furthermore, in the more general scenario where global classical correlations exist among all parties, quantum communication still outperforms classical methods. This result challenges the Frenkel–Weiner no-go theorem in the context of network communication. The observed quantum advantage is initially achieved through the use of entangled measurements by the receiver. Remarkably, we also show that entangled measurements are not necessary as separable measurements can also achieve similar quantum advantage. This finding broadens the scope of quantum advantage in network communication and highlights its robustness across different measurement paradigms.

## 3. Results

Consider the scenario where each sender transmits only 1 bit of classical information to the receiver to simulate a given MAC. Without local or SR, the parties must rely solely on classical deterministic strategies.

**Definition 1.** A classical deterministic strategy utilizing 1-bit communication from each sender to the receiver is defined by an ordered tuple $(\mathrm{E}_1, \cdots, \mathrm{E}_K, \mathrm{D})$, where $\mathrm{E}_i : X_i \mapsto \{0,1\}$ for $i \in \{1, \cdots, K\}$ maps the input set of the $i$th sender to a single bit, and $\mathrm{D} : \{0,1\}^K \mapsto A$ maps the bits received from all senders to the output set $A$.

By $\mathcal{E}_i$ we denote the set of all possible deterministic encodings for the $i$th sender, while $\mathcal{D}$ represents the set of all possible deterministic decodings for the receiver. The number of such strategies is finite whenever the sets $X_i$ and $A$ have finite cardinalities, and the set of all probability vectors obtained using such strategies, denoted as $\mathbf{C}_{\mathrm{ds}}^K$, forms a non-convex set in $\mathbb{R}^n$, where the exact value of $n$ depends on the cardinalities of the input and output sets. When each party randomizes their respective deterministic strategies locally, they implement a classical local strategy represented by the ordered tuple $(P(\mathcal{E}_1), \ldots, P(\mathcal{E}_K), P(\mathcal{D}))$ of probability distributions. Here, $P(\mathcal{E}_i)$ denotes the distribution over encoding functions, and $P(\mathcal{D})$ denotes the distribution over decoding functions. Set of all such strategies, denoted as $\mathbf{C}_{\mathrm{ls}}^K$, again forms a non-convex set. The introduction of SR among the parties enables them to employ correlated classical strategies.

**Definition 2.** A correlated classical strategy leverages classical SR and is represented by a probability distribution $P(\mathcal{E}_1 \times \cdots \times \mathcal{E}_K \times \mathcal{D})$ over the deterministic strategies.

For finite input–output cases, the collection of all correlated classical strategies, denoted as $\mathbf{C}_{\mathrm{cs}}^K$, forms a polytope embedded in $\mathbb{R}^n$. The extreme points of this polytope correspond to the deterministic strategies. Different physical configurations arise depending on the type of SR available. In definition 2, SR is permitted among all possible subgroups of the parties, and the SR resource in this configuration is denoted as $\$_G$. On the other hand, $\cup_{i=1}^K \$_{RS_i}$ denotes a configuration in which the receiver shares classical correlations with each sender independently (see figure 1)[5]. Unless specified otherwise, it will be assumed that an unlimited amount of SR is permitted among the parties within a designated subgroup. Strategies allowing SR among only some subgroups of parties form non-convex sets that lie strictly between $\mathbf{C}_{\mathrm{ls}}^K$ and $\mathbf{C}_{\mathrm{cs}}^K$. Moving to the quantum setup, with qubit communication, a quantum deterministic strategy is defined as follows.

**Definition 3.** A quantum deterministic strategy utilizing 1-qubit communication from each sender to the receiver is an ordered tuple $\left(\mathrm{E}_1^q, \cdots, \mathrm{E}_K^q, \mathrm{D}^q\right)$. Here, $\mathrm{E}_i^q : x_i \mapsto |\psi^{x_i}\rangle_{S_i} \in \mathbb{C}_{S_i}^2$ is the encoding strategy for the $i$th sender, mapping each input $x_i \in X_i$ to a qubit state $|\psi^{x_i}\rangle$. The decoding process is governed by $\mathrm{D}^q$, which is defined as $\{\Pi_l \in \mathbb{P}\left(\otimes_{i=1}^K \mathbb{C}_{S_i}^2\right) \mid \sum_{l=1}^{|A|} \Pi_l = \mathbf{I}\}$, representing a positive operator-valued measure (POVM) with $|A|$ outcomes that the receiver uses for decoding.

In definition 3, $\mathbb{P}(\mathcal{H})$ denotes the set of positive operators acting on the Hilbert space $\mathcal{H}$. The set of quantum deterministic strategies is denoted as $\mathbf{Q}_{\mathrm{ds}}^K$. Like $\mathbf{C}_{\mathrm{cs}}^K$, we can also define the set $\mathbf{Q}_{\mathrm{cs}}^K$, where each sender transmits one-qubit to the receiver and classical SR is available among them. For the case involving a single sender, with the input set denoted as $X$, the Frenkel–Weiner result implies that $\mathbf{Q}_{\mathrm{cs}}^1 = \mathbf{C}_{\mathrm{cs}}^1$ for all input cardinalities $|X|$ and output cardinalities $|A|$. This finding rules out any potential advantage of qubit communication over c-bit communication in the point-to-point communication scenario [9]. Interestingly, in the following, we establish that a Frenkel–Weiner kind of limitation theorem does not apply to MACs involving more than one sender. We substantiate this claim by demonstrating novel advantages of qubit communication over its classical counterpart in two-sender and three-sender MACs.

*Quantum advantages.–* Extending beyond the point-to-point communication framework, in our first example we examine a MAC comprising two senders and a single receiver. Each sender is assigned independent two-bit strings, $\mathbf{x} \in \{0,1\}^2$ and $\mathbf{y} \in \{0,1\}^2$, respectively, while the receiver generates a two-bit

[5] For clarity, consider the shared resource $\$_{S_1S_3R} \cup \$_{S_1S_5}$. While $\$_{S_1S_3R}$ enables $S_1$, $S_3$, and $R$ to correlate their encoding-decoding strategies, $S_1$ and $S_5$ can only correlate their encoding strategies through $\$_{S_1S_5}$. It is important to note that, given the resources $\$_{S_1S_3R} \cup \$_{S_1S_5}$, $S_3$ and $S_5$ cannot employ a correlated strategy.

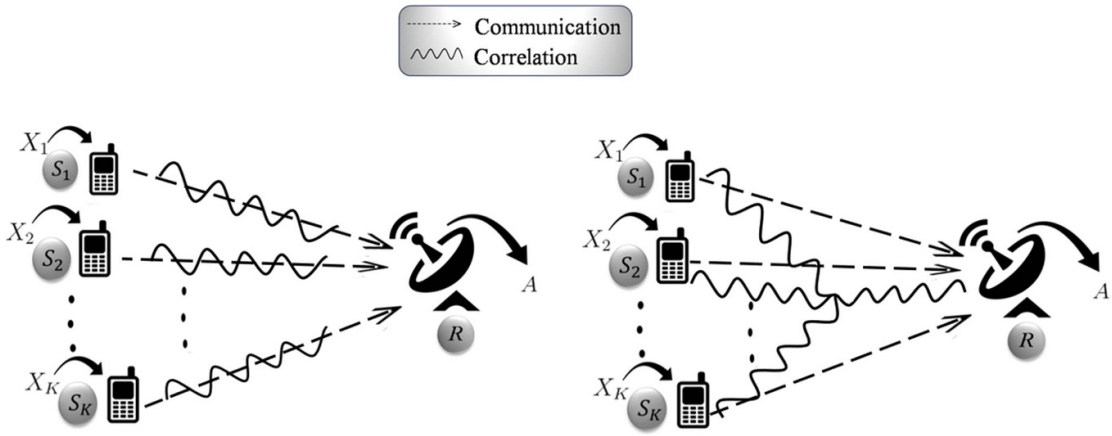


**Figure 1.** Multiple access channel with $K$ distant senders and one receiver, $\mathcal{N}^K \equiv \{p(a|x_1,\cdots,x_K) \mid a \in A,\ x_i \in X_i\}$. Left figure depicts each sender shares independent correlation with the receiver, whereas the right figure illustrates the global correlation shared among all senders and the receiver.

output string, $\mathbf{a} \in \{0,1\}^2$. The quantum strategy employed to reproduce the MAC is as follows: the senders respectively employ the encodings

$$\left\{\begin{matrix} \mathrm{E}_1^q : 00 \mapsto |0\rangle,\ 01 \mapsto |+\rangle,\ 10 \mapsto |-\rangle,\ 11 \mapsto |1\rangle \\ \mathrm{E}_2^q : 00 \mapsto |0\rangle,\ 01 \mapsto |-\rangle,\ 10 \mapsto |+\rangle,\ 11 \mapsto |1\rangle \end{matrix}\right\}; \tag{1}$$

where $\{|0\rangle,|1\rangle\}$ is the computational basis of $\mathbb{C}^2$, and $|\pm\rangle := (|0\rangle \pm |1\rangle)/\sqrt{2}$. The receiver performs a four-outcome two-qubit maximally entangled basis measurement on the qubits received from the senders:

$$\mathcal{M} := \left\{ |\psi_{ij}\rangle\langle\psi_{ij}|;\ |\psi_{ij}\rangle := \left(\mathbb{I}\otimes H^{1-j}X^{\overline{i\oplus j}}Z^{i\oplus j}\right)|\phi^+\rangle,\ i,j \in \{0,1\} \right\}$$

and decodes the two-bit outcome, denoted by $\mathbf{a}$, as '$i\ \overline{(i\oplus j)}$' when the projector $|\psi_{ij}\rangle\langle\psi_{ij}|$ clicks. Here, $|\phi^+\rangle := (|00\rangle + |11\rangle)/\sqrt{2}$, $H : |0\rangle\ (|1\rangle) \to |+\rangle\ (|-\rangle)$, and $X, Z$ are the Pauli gates. The resulting MAC can be compactly represented as, $\mathcal{N}^2_{\mathrm{PBR}} \equiv \left\{p(\mathbf{a}|\mathbf{x},\mathbf{y}) \mid \mathbf{a},\mathbf{x},\mathbf{y} \in \{0,1\}^2\right\}$, where

$$p\left(\mathbf{a}|\mathbf{x},\mathbf{y}\right) = \begin{cases} 1/2, & \text{when } \mathbf{a} = \mathbf{x}\oplus\mathbf{y}; \\ 0, & \text{when } \mathbf{a} = \overline{\mathbf{x}\oplus\mathbf{y}}; \\ 1/4, & \text{otherwise;} \end{cases} \tag{2}$$

$\mathbf{a} = \mathbf{x}\oplus\mathbf{y}$ denotes bit-wise XOR, i.e. $a_i = x_i \oplus y_i$ for $i = 1,2$ (explicit form of the stochastic matrix is provided in the appendix A). Notably, this quantum strategy draws inspiration from the renowned PBR theorem in quantum foundations [19], which in turn suggests the name $\mathcal{N}^2_{\mathrm{PBR}}$ for the resulting MAC. By construction, $\mathcal{N}^2_{\mathrm{PBR}}$ allows a simulation strategy in $\mathbf{Q}^2_{\mathrm{ds}}$. We now proceed to establish an impossibility result regarding simulation of this MAC with qubit communication replaced by its classical counterpart.

**Proposition 1.** *$\mathcal{N}^2_{\mathrm{PBR}}$ cannot be simulated using 1-bit communication from each sender to the receiver, even when the communication channels are supplemented with the classical SR of type $\$_{RS_1} \cup \$_{RS_2}$.*

**Proof.** (Outline) It is important to note that a limited number of conditional probabilities in $\mathcal{N}^2_{\mathrm{PBR}} \equiv \{p(\mathbf{a}|\mathbf{x},\mathbf{y})\}$ are zero. We begin by identifying the classical deterministic strategies that adhere to these zero conditions. Notably, only 48 deterministic strategies within $\mathbf{C}^2_{\mathrm{ds}}$ are compatible with these constraints. Subsequently, we demonstrate that any strategy derived from convex combinations of these 48 deterministic strategies, which reproduces $\mathcal{N}^2_{\mathrm{PBR}}$, necessitates that all three parties share global randomness $\$_G$ among themselves. This completes the proof, with comprehensive calculations detailed in the appendix A. □

Proposition 1 underscores the advantages of qubit communication over classical bits (c-bits) within a network communication framework. However, it is essential to recognize that the quantum advantage is somewhat constrained. While c-bit channels supplemented with the side resource $\cup_{i=1}^2 \$_{RS_i}$ are insufficient to simulate $\mathcal{N}^2_{\mathrm{PBR}}$, a classical strategy can be employed if the resource $\$_G$, i.e. global SR among the three parties, is permitted.

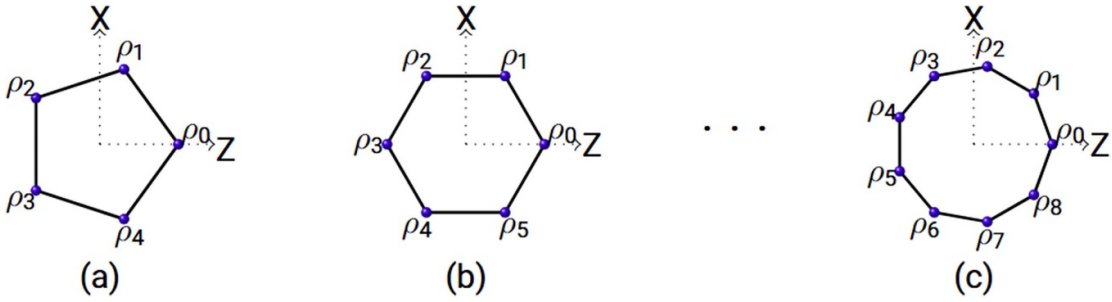


**Figure 2.** Encoding strategies in Polygon MACs ($m = 5, 6, \cdots, 9$). Upon receiving the input $u$, each sender prepares a qubit state $\rho_u = \frac{1}{2}\left(\mathbf{I} + \cos(2\pi u/m)\sigma_Z + \sin(2\pi u/m)\sigma_X\right)$ from the $XZ$ plane of the Bloch sphere and sends the encoded state to the receiver, where $m$ denotes the number of vertices of the polygon. Encoding for (a) pentagon-MAC ($m = 5$) (b) hexagon-MAC ($m = 6$), and (c) nonagon-MAC ($m = 9$) are shown above.

**Table 1.** Quantum advantage in simulating polygon-MAC.

| $\mathcal{N}_m^2$ | Classical bound ($k_m$) | Quantum value |
|---|---|---|
| $m = 5$ | $\mathbf{w}_5[\mathbf{p}_c] \leqslant 4$ | $15(\sqrt{5}-1)/4 \approx 4.63525$ |
| $m = 6$ | $\mathbf{w}_6[\mathbf{p}_c] \leqslant 6$ | 6.75 |
| $m = 7$ | $\mathbf{w}_7[\mathbf{p}_c] \leqslant 2$ | $\approx 2.61443$ |
| $m = 8$ | $\mathbf{w}_8[\mathbf{p}_c] \leqslant 8$ | $12\sqrt{2} - 8 \approx 8.97056$ |
| $m = 9$ | $\mathbf{w}_9[\mathbf{p}_c] \leqslant 2$ | $\approx 2.76003$ |

**Polygon MAC**: We now present a class of two-sender MACs that exhibit a more pronounced quantum advantage, where classical strategies become unattainable even with the inclusion of the side resource $\$_G$. In this setup, the senders receive inputs $x$ and $y$ from the set $\{0, \ldots, m-1\}$, while the receiver generates a binary output $a \in \{0, 1\}$. The probabilities $\{p(a = 0|x, y)\}$ uniquely characterize the MAC, as the other probability values are determined by normalization. Denoting $p(a = 0|x, y)$ as $p(x, y)$, we define the MAC $\mathcal{N}_m^2 \equiv \{p(x, y)\}$ as

$$\begin{aligned} &p(x,y) := \mathrm{Tr}\left[|\phi^+\rangle\langle\phi^+| \rho_x \otimes \rho_y\right], \\ &\text{where, } |\phi^+\rangle := \left(|00\rangle + |11\rangle\right)/\sqrt{2}, \\ &\text{and } \rho_u = \frac{1}{2}\left(\mathbf{I} + \cos\left(2\pi u/m\right)\sigma_Z + \sin\left(2\pi u/m\right)\sigma_X\right), \end{aligned} \tag{3}$$

for $u \in \{x, y\}$ (see figure 2). It follows from our construction that all these MACs can be effectively simulated using a quantum strategy based on qubit encoding. The encoding states reside on the vertices of an $m$-sided polygon situated in the $xz$-plane of the Bloch sphere, and we thus refer to them as polygon-MACs. Our next result demonstrates a more significant quantum advantage in simulating these polygon-MACs.

**Proposition 2.** *For $m \in \{5, \ldots, 9\}$, the polygon-MACs $\mathcal{N}_m^2$ cannot be simulated using the classical strategies $\mathbf{C}_{\mathrm{cs}}^2$.*

**Proof.** Since the set of strategies $\mathbf{C}_{\mathrm{cs}}^2$ is convex and compact, we can employ the classic Minkowski–Hahn–Banach hyperplane separation theorem from convex analysis. This theorem allows construction of a witness operator (or hyperplane) to check whether a given point lies within a convex compact set or not [24]. For each $m \in \{5, \ldots, 9\}$ we come up with the an explicit witness operator $\mathbf{w}_m$. Accordingly, for any strategy $\mathbf{p}_c \in \mathbf{C}_{\mathrm{cs}}^2$ the following inequality is satisfied

$$\mathbf{w}_m\left[\mathbf{p}_c\right] := \mathbf{w}_m \cdot \mathbf{p}_c = \sum_{x,y} w_m^{x,y} p_c(x,y) \leqslant k_m, \tag{4}$$

where $k_m$ denotes the optimal valued achieved through the strategies from the set $\mathbf{C}_{\mathrm{cs}}^2$, and it is determined by evaluating $\mathbf{w}_m[\mathbf{p}_c]$ for all deterministic strategies. Representing $\mathbf{w}_m \equiv (w_m^{x,y})$ as a matrix, with $w_m^{x,y}$ as the element in the $x$th row and $y$th column, the explicit forms of the witness operators are detailed in the appendix B. The quantum strategy, as defined in equation (3), yields a value exceeding $k_m$. The classical bounds and their corresponding quantum violations are summarized in table 1. This concludes the proof. □

The quantum advantages established in propositions 1 and 2 differ from those in communication complexity scenarios [25]. In communication complexity, the goal is to compute a function with inputs

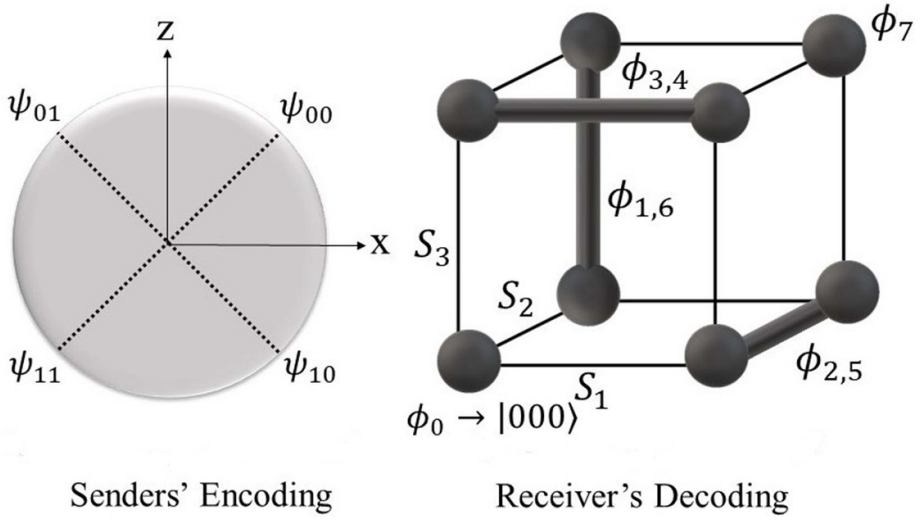


**Figure 3.** $\mathbf{Q}^3_{\text{ds}}$ strategy simulating the MAC $\mathcal{N}^3_{\text{shift}}$. While the encoding states are symmetrically chosen from the $xz$-plane of the Bloch sphere, the receiver employs the decoding measurement in SHIFT basis [20].

distributed among distant parties while minimizing communication among the parties. Examples of quantum advantages include quantum random access codes (RACs) [26–28], where non-classical properties are exploited in both encoding and decoding steps. The sender encodes the inputs in system's states prepared in quantum superposition (a nonclassical feature), while the receiver selects decoding measurements from a set of incompatible measurements (again a nonclassical feature). In Holevo and Frenkel–Weiner point-to-point communication, the lack of input to the receiver precludes the use of non-classical features at the decoding step. Nevertheless, propositions 1 and 2 demonstrate that quantum advantages can still be realized when multiple senders are involved. In such cases, the receiver can perform global measurements, such as entangled basis measurements, on the received quantum systems, thereby enabling these advantages.

Naturally, the question arises: is an entangled basis measurement necessary to achieve such an advantage? Interestingly, we will now demonstrate that this is not the case in general. For this, we consider a MAC involving three senders and one receiver. Each sender is provided with independent two-bit strings as inputs, $X, Y, Z \in \{0,1\}^{\times 2}$, while the receiver produces a three-bit string output $A \in \{0,1\}^{\times 3}$. Here, we adopt a reverse engineering approach to introduce the quantum strategy in $\mathbf{Q}^3_{\text{ds}}$ that leads to the desired MAC (see figure 3). The receiver employs a decoding measurement in a product basis known as the SHIFT ensemble, and we will refer to the resulting MAC as $\mathcal{N}^3_{\text{shift}}$. The resulting MAC can be expressed compactly as

$$\mathcal{N}^3_{\text{shift}} \equiv \left\{ p(\mathbf{a}|\mathbf{x},\mathbf{y},\mathbf{z}) = \zeta_+^{\eta}\zeta_-^{(3-\eta)} \right\}, \tag{5}$$

$$\mathbf{x},\mathbf{y},\mathbf{z} \in \{0,1\}^{\times 2},\ \mathbf{a} \in \{0,1\}^{\times 3},\ \zeta_\pm := \frac{1}{2}\left(1 \pm \frac{1}{\sqrt{2}}\right),$$

$$\text{where, } p(\mathbf{a}|\mathbf{x},\mathbf{y},\mathbf{z}) := 2\delta_{3,\eta} - 3\delta_{2,\eta} - 2\delta_{1,\eta} - 2\delta_{0,\eta},$$

$$\eta := \begin{cases} \delta_{x_1,a_1} + \delta_{y_1,a_2} + \delta_{z_1,a_3}, & \text{if } a_1 = a_2 = a_3, \\ \delta_{x_1,0} + \delta_{y_1,1} + \delta_{z_2,a_3}, & \text{if } a_1 = a_2 \neq a_3, \\ \delta_{x_1,1} + \delta_{y_2,a_2} + \delta_{z_1,0}, & \text{if } a_3 = a_1 \neq a_2, \\ \delta_{x_2,a_1} + \delta_{y_1,0} + \delta_{z_1,1}, & \text{if } a_2 = a_3 \neq a_1. \end{cases} \tag{6}$$

Here, $\delta$ denotes the Kronecker Delta symbol. Notably, the SHIFT measurement demonstrates the phenomenon of 'quantum nonlocality without entanglement' (QNWE) [20] (see also [29]), and its implementation requires a global interaction among the three qubits [30]. Our next result establishes that $\mathcal{N}^3_{\text{shift}}$ cannot be simulated using the corresponding classical strategies.

**Proposition 3.** *The MAC $\mathcal{N}^3_{\text{shift}}$ cannot be simulated using any strategy from the set $\mathbf{C}^3_{\text{cs}}$.*

**Proof.** Denoting the input string as $\mathbf{s} = s_1 s_2$, encoding states of the respective senders are given by

$$\psi_{\mathbf{s}} \equiv |\psi_{\mathbf{s}}\rangle\langle\psi_{\mathbf{s}}| = \frac{1}{2}\left[\mathbf{I} + \frac{(-1)^{s_1}}{\sqrt{2}}\sigma_Z + \frac{(-1)^{s_2}}{\sqrt{2}}\sigma_X\right], \tag{7}$$

where $\mathbf{s} \in \{\mathbf{x}, \mathbf{y}, \mathbf{z}\}$. It is important to note that the encoding states are symmetrically chosen from the $xz$-plane of the Bloch sphere. For decoding, the receiver performs SHIFT basis measurement [20] on the three qubits received from the senders and decodes the outcome according to the following strategy:

$$\left\{\begin{array}{ll} |\phi_0\rangle := |000\rangle \mapsto 000, & |\phi_1\rangle := |01-\rangle \mapsto 001, \\ |\phi_2\rangle := |1-0\rangle \mapsto 010, & |\phi_3\rangle := |+01\rangle \mapsto 011, \\ |\phi_4\rangle := |-01\rangle \mapsto 100, & |\phi_5\rangle := |1+0\rangle \mapsto 101, \\ |\phi_6\rangle := |01+\rangle \mapsto 110, & |\phi_7\rangle := |111\rangle \mapsto 111 \end{array}\right\}. \tag{8}$$

The $8 \times 64$ stochastic matrix of $\mathcal{N}^3_{shift}$ has some interesting symmetry. To note this symmetry, consider the case where all the senders have input '0', i.e., $x = y = z = 00$. The probabilities of different outcomes at the receiver's end read as:

$$\left\{\begin{array}{l} p(000) = \zeta_+^3, \;\; p(011) = p(101) = p(110) = \zeta_+^2\zeta_- \\ p(001) = p(010) = p(100) = \zeta_-^2\zeta_+, \;\; p(111) = \zeta_-^3, \end{array}\right\},$$

where $\zeta_\pm := \frac{1}{2}(1 \pm \frac{1}{\sqrt{2}})$. In other words, exactly one outcome occurs with probability $\zeta_+^3$, exactly three occur with probability $\zeta_-^2\zeta_+$, exactly three occur with probability $\zeta_-\zeta_+^2$, and the remaining one occurs with probability $\zeta_-^3$.Interestingly, for any of the input-triples $(x, y, z) \in \{0,1\}^{\times 2} \times \{0,1\}^{\times 2} \times \{0,1\}^{\times 2}$, exactly the same pattern with the same probabilities hold (we call it the "$1-3-3-1$" pattern). Thus, each of the columns of this $8 \times 64$ Stochastic matrix $\mathcal{N}^3_{\text{shift}}$ are identical up-to some permutation of the rows. Consider now a witness operator $\mathbf{W}_{\text{shift}} \equiv \{W_{\mathbf{a}|\mathbf{x},\mathbf{y},\mathbf{z}} \mid \mathbf{x}, \mathbf{y}, \mathbf{z} \in \{0,1\}^{\times 2},\ \mathbf{a} \in \{0,1\}^{\times 3}\}$, where

$$W_{\mathbf{a}|\mathbf{x},\mathbf{y},\mathbf{z}} := 2\delta_{3,\eta} - 3\delta_{2,\eta} - 2\delta_{1,\eta} - 2\delta_{0,\eta} \;\; . \tag{9}$$

Here, $\eta$ is as defined in equation (6). We now proceed to evaluate the value of $\mathcal{N}^3_{\text{shift}}$ for this witness operation, which becomes

$$\begin{aligned} \mathbf{W}_{\text{shift}}\left[\mathcal{N}^3_{\text{shift}}\right] &\equiv \mathbf{W}_{\text{shift}} \cdot \mathcal{N}^3_{\text{shift}} \\ &:= \sum_{\mathbf{x},\mathbf{y},\mathbf{z},\mathbf{a}} W_{\mathbf{a}|\mathbf{x},\mathbf{y},\mathbf{z}} \times p(\mathbf{a}|\mathbf{x},\mathbf{y},\mathbf{z}) \\ &= \sum_{\mathbf{x},\mathbf{y},\mathbf{z}} \left\{ \sum_{\mathbf{a}} W_{\mathbf{a}|\mathbf{x},\mathbf{y},\mathbf{z}} \times p(\mathbf{a}|\mathbf{x},\mathbf{y},\mathbf{z}) \right\} \\ &= \sum_{\mathbf{x},\mathbf{y},\mathbf{z}} \left\{ \sum_{\eta=0}^{3} [1 \times (+2)\,\delta_{3,\eta} + 3 \times (-3)\,\delta_{2,\eta} \right. \\ &\qquad \left. +3 \times (-2)\,\delta_{1,\eta} + 1 \times (-2)\,\delta_{0,\eta}] \times \zeta_+^{\eta}\zeta_-^{(3-\eta)} \right\} \\ &= \sum_{\mathbf{x},\mathbf{y},\mathbf{z}} \left\{ 2\zeta_+^3 - 9\zeta_+^2\zeta_- - 6\zeta_-^2\zeta_+ - 2\zeta_-^3 \right\} \\ &= 64 \times \left\{ 2\zeta_+^3 - 9\zeta_+^2\zeta_- - 6\zeta_-^2\zeta_+ - 2\zeta_-^3 \right\} \\ &= 10\left(5\sqrt{2} - 6\right) \approx 10.7107\,. \end{aligned} \tag{10}$$

To establish the quantum advantage we are now left to show that any strategy in $\mathbf{C}^3_{\text{cs}}$ yields a value lower than quantum value for the witness operator $\mathbf{W}_{\text{shift}}$. In appendix C we systematically analyze all the deterministic classical strategies and show that the classical values are upper bounded by 8. This completes the proof. □

Proposition 3 offers an additional insight. As noted by Bennett and Shor [31], depending on whether product or entangled states are used at the input, and product or entangled measurements are performed at the output, the classical capacity of a quantum channel can be defined in four different ways. While all of them are the same for perfect quantum channels, for noisy channels a distinct advantage can be obtained invoking entanglement at encoding and decoding steps, enhancing capacity beyond that achievable with product encoding and product decoding [32–34]. However, when product decoding is used, this advantage vanishes, even if entangled states are employed in encoding [35]. Notably, proposition 3 demonstrates that a product-basis measurement exhibiting QNWE can still be advantageous for simulating a MAC.

At this point, we end by noting down another important observation.

**Observation 1.** The MACs $\mathcal{N}^2_{\text{PBR}}$, $\mathcal{N}^3_{\text{shift}}$, and $\mathcal{N}^2_m$ can all be simulated using 1-cbit communication from each sender to the receiver, provided each communication line is assisted by a two-qubit maximally entangled state.

This observation follows directly from the well-known 'remote state preparation' (RSP) protocol [36–38]. In all cases, the encoding states are selected from great circles on the Bloch sphere, as prescribed by the RSP protocol. Using a maximally entangled state shared with the receiver, the senders can remotely prepare the encoding states at the receiver's end by transmitting just 1 bit of classical communication. The decoding step then proceeds as in qubit-based protocols.

## 4. Noise-robustness of the quantum advantage

Noise is an unavoidable challenge in any communication channel, and its impact becomes even more critical in quantum systems. Even a tiny thermal noise can disrupt the encoded quantum information. Additionally, the decoding measurement can be noisy making it difficult to achieve the targeted goal. Therefore, it is essential to explore whether the quantum advantage holds up in noisy conditions. In this context, we focus primarily on the polygon MAC, although similar analyses can be extended to other scenarios as well. Depolarizing noise ($D$) is a type of noise that affects the entire Bloch sphere uniformly. This noise can occur experimentally when Alice is unable to create perfect quantum states, ideally represented as

$$\rho_k = \frac{1}{2}\left[\mathbb{I} + \hat{n}_k \cdot \vec{\sigma}\right].$$

Instead, the vector $\hat{n}_k$ is uniformly distributed within a cone on the Bloch sphere, which subtends a solid angle $\Omega$ at the origin and is aligned along the axis $\hat{n}_k$. (see figure 4). For such a noise $D^\epsilon$, specified by depolarizing parameter $\epsilon \in [0,1]$, a state $\rho_k = \frac{1}{2}[\mathbb{I} + \hat{n}_k.\vec{\sigma}]$ gets modified as

$$\begin{aligned} D^\epsilon(\rho_k) &:= (1-\epsilon)\rho_k + \epsilon\frac{\mathbb{I}}{2} = \frac{1}{2}\left[\mathbb{I} + (1-\epsilon)\hat{n}_k.\vec{\sigma}\right] \\ &= \frac{1}{2}\left[\mathbb{I} + D^\epsilon(\hat{n}_k).\vec{\sigma}\right], \;\; D^\epsilon(\hat{n}_k) := (1-\epsilon)\hat{n}_k. \end{aligned} \tag{11}$$

Similarly, the POVM element $|\phi^+\rangle\langle\phi^+|$ get modified to,

$$D^\epsilon \otimes D^\epsilon\left(|\phi^+\rangle\langle\phi^+|\right) := (1-\epsilon)^2|\phi^+\rangle\langle\phi^+| + \epsilon(2-\epsilon)\frac{\mathbb{I}}{2}\otimes\frac{\mathbb{I}}{2}. \tag{12}$$

We, know that the ideal encoding and decoding protocol results in $p(x,y) := \text{Tr}\left[|\phi^+\rangle\langle\phi^+|\rho_x \otimes \rho_y\right]$ (equation (3)). Now consider that both the sender's encoding protocol undergoes the same depolarizing noise $D^\epsilon_S$. The receiver's decoding, let us say, gets affected with depolarizing noise $D^\epsilon_R$. Hence, the modified probability reads as

$$\begin{aligned} p_{\text{noisy}}(x,y) :=& \text{Tr}\Big[D^\epsilon_R \otimes D^\epsilon_R(|\phi^+\rangle\langle\phi^+|)\left(D^\epsilon_S(\rho_x)\otimes D^\epsilon_S(\rho_y)\right)\Big] \\ =& \text{Tr}\Big[\Big\{(1-\epsilon_R)^2|\phi^+\rangle\langle\phi^+| + \epsilon_R(2-\epsilon_R)\frac{\mathbb{I}}{2}\otimes\frac{\mathbb{I}}{2}\Big\} \\ & \cdot\frac{1}{2}\Big\{\mathbf{I} + (1-\epsilon_S)\left(\cos(2\pi x/m)\sigma_Z + \sin(2\pi x/m)\sigma_X\right)\Big\} \\ & \otimes\frac{1}{2}\Big\{\mathbf{I} + (1-\epsilon_S)\left(\cos(2\pi y/m)\sigma_Z + \sin(2\pi y/m)\sigma_X\right)\Big\}\Big]. \end{aligned}$$

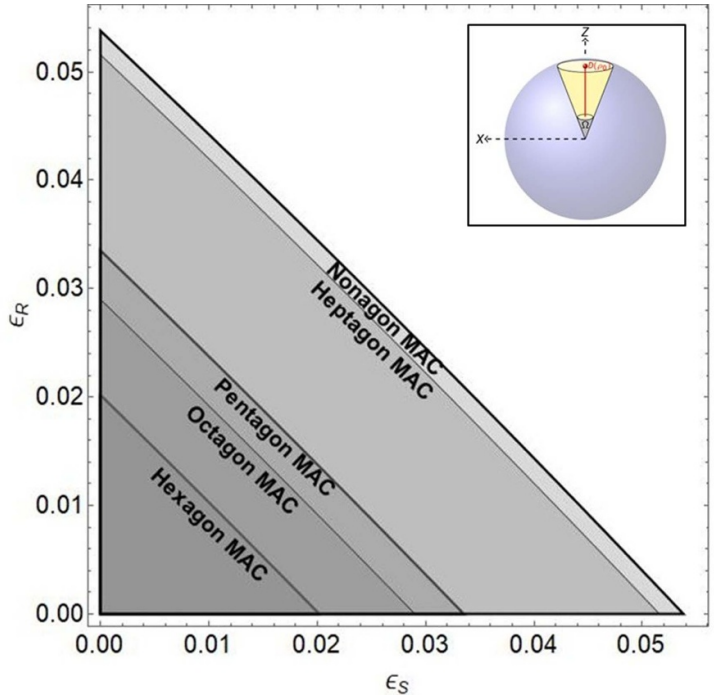


**Figure 4.** The noise robustness for different polygon MACs is shown in the above figure. (Inset) When subjected to depolarizing noise, the encoded states contract within the Bloch sphere. It is assumed that both the encoded states and the decoding effects are affected by this noise in a similar manner.

With the encoding and decoding protocol for the polygon MAC unchanged, in the presence of depolarizing noise at the encoding and decoding site, we find a range wherein there is a quantum advantage over the classical bound as listed in table 1. See figure 4 which captures the noise robustness of the various polygon MACs.

## 5. Discussions

Quantum advantages are elusive, challenging to establish, and often constrained by fundamental no-go theorems. For instance, while quantum computing can offer speedups over classical computers for certain problems, the set of functions computable by quantum mechanics remains identical to those computable by classical physics. Similarly, in point-to-point communication, the Holevo–Frenkel–Weiner results limit the usefulness of quantum systems when no entanglement is shared between sender and receiver. However, in this work, we demonstrate that such limitations do not apply in a network communication setting. Specifically, in simulating multiple-sender-to-one-receiver channels, our study reveals a novel advantage of qubit communication over the corresponding classical resources. Notably, this advantage is distinct from recent studies on MACs [39–41], which show that nonlocal correlations shared among distant senders can increase channel capacities. As noted, our construction in Proposition 1 is inspired by the PBR theorem, which asserts the $\psi$-ontic nature of quantum wavefunctions, implying a direct correspondence with physical reality [42]. Exploring a deeper link between the $\psi$-onticity of wavefunctions and the quantum advantage reported here would be fascinating.

It is important to note that the quantum advantages in propositions 1 and 2 do not depend on incompatible measurements at the decoding stage; instead, they involve measurements using entangled projectors. Such measurements are known to be crucial in the phenomenon of 'quantum-nonlocality-without-inputs' [43]. Investigating the connection between this quantum advantage and network nonlocality [44] is a promising direction for future work. Moreover, our construction provides a pathway for semi-device-independent certification of entangled measurements [45–47]. In particular, in the polygon MAC, it is worth exploring the optimal violation of the respective witness operations when Bob performs a two-qubit product basis measurement on the encoded states received from the senders. By assuming the encoding processes to be trusted while treating the decoding process as a black box, violations of these threshold values would constitute a semi-device-independent certification of entangled measurements. Proposition 3 further highlights the critical role of QNWE in establishing qubit advantages over classical bits

in network communication scenarios. Many other product bases exhibiting QNWE have been documented, with recent studies introducing various new variants of this phenomenon [48–50]. Exploring these constructions to establish quantum advantages in MAC scenarios would be highly interesting.

The physical implementation of the proposed protocols necessitates the preparation of pure qubit states. Given the inherent fragility of quantum states, one approach is to utilize the quantum state purification protocol proposed in [51], which has been experimentally demonstrated in [52]. This purification process enhances the fidelity of the quantum states, making them more robust for subsequent operations. Implementation of PBR MAC and polygon MACs further requires the capability to perform entanglement basis measurements, a technique that has already been realized across various quantum architectures, including photonic systems, silicon processor, and trapped ions [53–57]. These existing experimental advancements provide a solid foundation for realizing the protocols discussed. However, several loopholes must be addressed to demonstrate the reported quantum advantage in experiments. Firstly, the *locality loophole*-in our setup, we assume no communication among the distant senders. This can be addressed by ensuring that the encoding events of different senders are spacelike separated. Additionally, we assume the *freedom of choice* assumption, which ensures that the inputs sent to different senders are independent. Furthermore, when implementing the protocol in photonic architectures, one must also address the *detection loophole*.

## Data availability statement

All data that support the findings of this study are included within the article (and any supplementary files).

## Acknowledgments

EPL is grateful to Stefano Pironio for discussions on numerical methods. We gratefully acknowledge the private communication with Qiang Zhang and Chen Zhuoran of University of Science and Technology of China for pointing out the possible loopholes that might arise during experimental implementation of the reported quantum advantage. SGN acknowledges support from the CSIR Project 09/0575(15951)/2022-EMR-I. EPL acknowledges funding from the QuantERA II Programme that has received funding from the European Union's Horizon 2020 research and innovation programme under Grant Agreement No 101017733 and the F.R.S-FNRS Pint-Multi programme under Grant Agreement R.8014.21, from the European Union's Horizon Europe research and innovation programme under the project 'Quantum Security Networks Partnership' (QSNP, Grant Agreement No 101114043), from the F.R.S-FNRS through the PDR T.0171.22, from the FWO and F.R.S.-FNRS under the Excellence of Science (EOS) programme Project 40007526, from the FWO through the BeQuNet SBO Project S008323N, from the Belgian Federal Science Policy through the contract RT/22/BE-QCI and the EU 'BE-QCI' program. E.P.L. acknowledges support from the Fonds de la Recherche Scientifique – FNRS through a FRIA grant. EPL is funded by the European Union. Views and opinions expressed are however those of the author only and do not necessarily reflect those of the European Union. The European Union cannot be held responsible for them. MA acknowledges the funding supported by the European Union (Project QURES- GA No. 101153001). MB acknowledges funding from the National Mission in Interdisciplinary Cyber-Physical systems from the Department of Science and Technology through the I-HUB Quantum Technology Foundation (Grant No: I-HUB/PDF/2021-22/008).

## Appendix A. Proof of proposition 1

Represented as a stochastic matrix, the MAC $\mathcal{N}^2_{\mathrm{PBR}}$ reads as

$\mathcal{N}^2_{\mathrm{PBR}} \equiv$

| $\mathbf{a}\backslash\mathbf{x},\mathbf{y}$ | 00, 00 | 00, 01 | 00, 10 | 00, 11 | 01, 00 | 01, 01 | 01, 10 | 01, 11 | 10, 00 | 10, 01 | 10, 10 | 10, 11 | 11, 00 | 11, 01 | 11, 10 | 11, 11 |
|---|---|---|---|---|---|---|---|---|---|---|---|---|---|---|---|---|
| 00 | 1/2 | 1/4 | 1/4 | 0 | 1/4 | 1/2 | 0 | 1/4 | 1/4 | 0 | 1/2 | 1/4 | 0 | 1/4 | 1/4 | 1/2 |
| 01 | 1/4 | 1/2 | 0 | 1/4 | 1/2 | 1/4 | 1/4 | 0 | 0 | 1/4 | 1/4 | 1/2 | 1/4 | 0 | 1/2 | 1/4 |
| 10 | 1/4 | 0 | 1/2 | 1/4 | 0 | 1/4 | 1/4 | 1/2 | 1/2 | 1/4 | 1/4 | 0 | 1/4 | 1/2 | 0 | 1/4 |
| 11 | 0 | 1/4 | 1/4 | 1/2 | 1/4 | 0 | 1/2 | 1/4 | 1/4 | 1/2 | 0 | 1/4 | 1/2 | 1/4 | 1/4 | 0 |

As it turns out few of the conditional probabilities in $\mathcal{N}^2_{\mathrm{PBR}}$ are zero. In particular

$$p(\mathbf{a}|\mathbf{x},\mathbf{y}) = 0, \quad \text{when } a_1 = \overline{x_1 \oplus y_1} \ \wedge \ a_2 = \overline{x_2 \oplus y_2}. \tag{A1}$$

**Table 2.** An instance of disallowed encoding.

| $\alpha\beta$ | $x_1x_2$ | $y_1y_2$ | $x_1 \oplus y_1$ | $x_2 \oplus y_2$ | $\overline{x_1 \oplus y_1}\ \overline{x_2 \oplus y_2}$ |
|---|---|---|---|---|---|
| 00 | 00 | 00 | 0 | 0 | 11 |
| | 00 | 01 | 0 | 1 | 10 |
| | 00 | 10 | 1 | 0 | 01 |
| | 01 | 00 | 0 | 1 | 10 |
| | 01 | 01 | 0 | 0 | 11 |
| | 01 | 10 | 1 | 1 | 00 |

A classical deterministic strategy $\mathcal{S} \equiv (\mathrm{E}_1, \mathrm{E}_2, \mathrm{D}) \in \mathbf{C}^2_{\mathrm{ds}}$ aiming to simulate $\mathcal{N}^2_{\mathrm{PBR}}$ must satisfy these requirements. Let us denote the deterministic encodings by the senders and decoding by the receiver as below

$$\mathrm{E}_1 :\ \{0,1\}^{\otimes 2} \ni \mathbf{x} \equiv x_1x_2 \mapsto \alpha \in \{0,1\}\,, \tag{A2a}$$

$$\mathrm{E}_2 :\ \{0,1\}^{\otimes 2} \ni \mathbf{y} \equiv y_1y_2 \mapsto \beta \in \{0,1\}\,, \tag{A2b}$$

$$\mathrm{D} :\ \alpha \times \beta \mapsto \mathbf{a} \equiv a_1a_2 \in \{0,1\}^{\times 2}\,. \tag{A2c}$$

The following observations are crucial.

**Observation 2.** For the fixed encoding strategies employed by the senders, the conditions in equation (A1) impose constraints on the permissible decoding strategies at the receiver's end. For example, if the senders utilize the encoding method

$$\mathrm{E}_1 :\ 00 \mapsto 0\ \&\ \{01,10,11\} \mapsto 1; \tag{A3a}$$

$$\mathrm{E}_2 :\ 00 \mapsto 0\ \&\ \{01,10,11\} \mapsto 1. \tag{A3b}$$

The receiver cannot employ the decoding strategies $\mathrm{D} : 00 \mapsto 11$, as it yields $p(11|00,00) = 1$, a violation of the requirement (A1). Therefore, for the given encoding this particular decoding is not allowed.

**Observation 3.** For certain encoding strategies, there does not exist any decoding strategy compatible with the requirement (A1). To see an explicit example, consider the following encodings

$$\mathrm{E}_1 :\ \{00,01\} \mapsto 0\ \&\ \{10,11\} \mapsto 1; \tag{A4a}$$

$$\mathrm{E}_2 :\ \{00,01,10\} \mapsto 0\ \&\ 11 \mapsto 1. \tag{A4b}$$

In table 2, we analyze the case when the receiver gets $\alpha = 0$ and $\beta = 0$ from the two senders, respectively. While decoding, the message $\alpha\beta = 00$ must be decoded as one of four possible outcomes $\mathbf{a} = a_1a_2 \in \{0,1\}^{\times 2}$. As evident from the last column of table 2, whatever output is decoded for the message $\alpha\beta = 00$ the condition (A1) gets violated.

These observations lead us to the following general lemma.

**Lemma 1.** *Encoding strategics where the four inputs are grouped in two disjoint set with equal cardinalities for both the senders are the only possible encodings compatible for simulating the MAC* $\mathcal{N}^2_{\mathrm{PBR}}$.

**Proof.** A generic encoding, $\mathrm{E}_1 : \mathbf{x} \mapsto \alpha$, employed by the sender $S_1$ (and similarly for the sender $S_2$) is a partition of the input strings $\mathbf{x} \in \{0,1\}^{\times 2}$ into two disjoint sets $\mathbf{x}^\alpha$, i.e.

$$\mathbf{x} = \mathbf{x}^0 \cup \mathbf{x}^1,\ \text{ such that }\ \mathbf{x}^0 \cap \mathbf{x}^1 = \emptyset. \tag{A5}$$

Let, cardinalities of the sets $\mathbf{x}^0$ and $\mathbf{x}^1$ be $\mathbf{c}$ and $4-\mathbf{c}$, respectively, with $\mathbf{c} \in \{0,1,2,3,4\}$. As the partitions with $|\mathbf{x}^0| = \mathbf{c}$ and $|\mathbf{x}^0| = 4-\mathbf{c}$ are same under relabeling, it is thus sufficient to analyze the cases $\mathbf{c} \in \{0,1,2\}$.

Let us first consider the case where $|\mathbf{x}^0| = 2$ and $|\mathbf{y}^0| = 1$. The first sender can employ one of the following strategies,

$$\mathrm{e}^1 := \mathrm{E}^{1\mathrm{st}}_{\mathrm{bit}} : \{00,01\} \mapsto 0,\quad \{10,11\} \mapsto 1; \tag{A6a}$$

$$\mathrm{e}^2 := \mathrm{E}^{2\mathrm{nd}}_{\mathrm{bit}} : \{00,10\} \mapsto 0,\quad \{01,11\} \mapsto 1; \tag{A6b}$$

$$\mathrm{e}^3 := \mathrm{E}_{\mathrm{par}} : \{00,11\} \mapsto 0,\quad \{01,10\} \mapsto 1; \tag{A6c}$$

**Table 3.** Allowed decoding strategies for the encoding $\mathrm{E}_1 = \mathrm{e}^1 = \mathrm{E}_2$.

| $\alpha\beta$ | $x_1x_2$ | $y_1y_2$ | $x_1 \oplus y_1$ | $x_2 \oplus y_2$ | $\overline{x_1 \oplus y_1}\ \overline{x_2 \oplus y_2}$ | Compatible Decoding $a_1a_2$ |
|---|---|---|---|---|---|---|
| 00 | 00 | 00 | 0 | 0 | 11 | 00 or 01 |
| | 00 | 01 | 0 | 1 | 10 | |
| | 01 | 00 | 0 | 1 | 10 | |
| | 01 | 01 | 0 | 0 | 11 | |
| 01 | 00 | 10 | 1 | 0 | 01 | 11 or 10 |
| | 00 | 11 | 1 | 1 | 00 | |
| | 01 | 10 | 1 | 1 | 00 | |
| | 01 | 11 | 1 | 0 | 01 | |
| 10 | 10 | 00 | 1 | 0 | 01 | 11 or 10 |
| | 10 | 01 | 1 | 1 | 00 | |
| | 11 | 00 | 1 | 1 | 00 | |
| | 11 | 01 | 1 | 0 | 01 | |
| 11 | 10 | 10 | 0 | 0 | 11 | 00 or 01 |
| | 10 | 11 | 0 | 1 | 10 | |
| | 11 | 10 | 0 | 1 | 10 | |
| | 11 | 11 | 0 | 0 | 11 | |

and the encoding of the second sender can be represented as

$$\mathrm{E}^{1|3}_{i,j} : ij \mapsto 0, \quad \{\bar{i}j, i\bar{j}, \bar{i}\bar{j}\} \mapsto 1, \quad \text{where } i,j \in \{0,1\}. \tag{A7}$$

As it turns out, whatever encodings are followed by the senders, a situation like Observation 3 arises. Same will be the case whenever $|\mathbf{x}^0| = 1$ & $|\mathbf{y}^0| = 2$ as well as $|\mathbf{x}^0| < 2$ & $|\mathbf{y}^0| < 2$. This concludes the proof. □

Among the allowed encodings $\mathrm{E}_1, \mathrm{E}_2 \in \{\mathrm{e}^1, \mathrm{e}^2, \mathrm{e}^3\}$, following observations are further relevant.

**Observation 4.** There does not exist a valid decoding compatible with (A1) whenever the senders employ encoding $\mathrm{E}_1 = \mathrm{e}^u$ and $\mathrm{E}_2 = \mathrm{e}^v$, with $u \neq v$ and $u, v, \in \{1,2,3\}$.

**Observation 5.** For each of the encoding $\mathrm{E}_1 = \mathrm{e}^u = \mathrm{E}_2$, there are 16 possible decoding $\mathrm{d}^w_u$ leading to valid strategies $\mathcal{S}^{uw} \equiv (\mathrm{e}^u, \mathrm{e}^u, \mathrm{d}^w_u)$ that are compatible with (A1); $u \in \{1,2,3\}$ and $w \in \{1, \cdots, 16\}$. For instance, for the encoding $\mathrm{E}_1 = \mathrm{e}^1 = \mathrm{E}_2$ the allowed decoding strategies are listed in table 3.

**Remark 1.** The senders and receiver can further employ a strategy $\mathcal{S}^u[p_w] = \sum_w p_w \mathcal{S}^{uw}$, where $\{p_w\}_w$ denotes a probability distribution. Such a strategy can be employed using local randomness at receiver's end. As we note, none of these strategies can simulate the MAC $\mathcal{N}^2_{\mathrm{PBR}}$. This can also be argued with simple reasoning. In this strategy, the encoding of the sender is fixed and there are only 16 compatible decoding strategies exist. Any communication $\alpha\beta$ can be decoded into two possible outcomes which in turn leads to the impossibility of the simulation of MAC $\mathcal{N}^2_{\mathrm{PBR}}$. For instance, it is clear from the above table that mixing all compatible decoding strategies for this fixed encoding will results in $p(10|00,00) = 0$.

**Remark 2.** The senders and receiver can also employ a strategy $\mathcal{S}[p_{uw}] = \sum_{uw} p_{uw} \mathcal{S}^{uw}$, where $\{p_{uw}\}_{uw}$ denotes classical correlation shared among the senders and receiver. As it turns out the strategy $\mathcal{S}[\frac{1}{32}] = \sum_{u=1}^{2} \sum_{w=1}^{16} \frac{1}{32} \mathcal{S}^{uw}$ simulates the MAC $\mathcal{N}^2_{\mathrm{PBR}}$. Importantly, this strategy cannot be implemented through 1-cbit channel from each sender to the receiver assisted with SR resource $\$_{RS_1} \cup \$_{RS_1}$. However, it can be implemented if the resource $\$_G$ is allowed to be shared.

## Appendix B. Proof of proposition 2

Witness operators for the polygon MAC are analogous to Bell-type inequalities for the space-like separated scenario. Here we construct linear inequalities for each $m \in \{5, \cdots, 9\}$. For a given strategy $\mathbf{p}_c \in \mathbf{C}^2_{\text{cs}}$ , the inequality is given by

$$\mathbf{w}_m\left[\mathbf{p}_c\right] := \mathbf{w}_m \cdot \mathbf{p}_c := \sum_{x,y} w_m^{x,y} p_c\left(x,y\right) \leqslant k_m, \tag{B1}$$

$$\mathbf{w}_5 = \begin{bmatrix} 0 & 1 & -3 & -5 & 3 \\ 3 & 0 & 1 & -3 & -5 \\ -5 & 3 & 0 & 1 & -3 \\ -3 & -5 & 3 & 0 & 1 \\ 1 & -3 & -5 & 3 & 0 \end{bmatrix}; \quad \mathbf{w}_6 = \begin{bmatrix} 0 & 4 & -4 & -4 & -5 & 2 \\ 2 & 0 & 4 & -4 & -4 & -2 \\ -5 & 2 & 0 & 4 & -7 & -10 \\ -4 & -5 & 2 & 0 & 4 & -4 \\ -4 & -4 & -2 & 2 & 0 & 4 \\ 4 & -7 & -4 & -5 & 2 & 0 \end{bmatrix};$$

$$\mathbf{w}_7 = \begin{bmatrix} 0 & 1 & -1 & -1 & -1 & -1 & 1 \\ 1 & 0 & 1 & -1 & -1 & -1 & -1 \\ -1 & 1 & 0 & 1 & -1 & -1 & -1 \\ -1 & -1 & 1 & 0 & 1 & -1 & -1 \\ -1 & -1 & -1 & 1 & 0 & 1 & -1 \\ -1 & -1 & -1 & -1 & 1 & 0 & 1 \\ 1 & -1 & -1 & -1 & -1 & 1 & 0 \end{bmatrix}; \quad \mathbf{w}_8 = \begin{bmatrix} 0 & 0 & 0 & 0 & 0 & 0 & 0 & 0 \\ 1 & 0 & 7 & 0 & -11 & 0 & -5 & 0 \\ 0 & 0 & 0 & 0 & 0 & 0 & 0 & 0 \\ -5 & 0 & 1 & 0 & 7 & 0 & -11 & 0 \\ 0 & 0 & 0 & 0 & 0 & 0 & 0 & 0 \\ -11 & 0 & -5 & 0 & 1 & 0 & 7 & 0 \\ 0 & 0 & 0 & 0 & 0 & 0 & 0 & 0 \\ 7 & 0 & -11 & 0 & -5 & 0 & 1 & 0 \end{bmatrix};$$

$$\mathbf{w}_9 = \begin{bmatrix} 0 & 0 & 1 & -1 & -1 & -1 & -1 & 1 & 0 \\ 0 & 0 & 0 & 1 & -1 & -1 & -1 & -1 & 1 \\ 1 & 0 & 0 & 0 & 1 & -1 & -1 & -1 & -1 \\ -1 & 1 & 0 & 0 & 0 & 1 & -1 & -1 & -1 \\ -1 & -1 & 1 & 0 & 0 & 0 & 1 & -1 & -1 \\ -1 & -1 & -1 & 1 & 0 & 0 & 0 & 1 & -1 \\ -1 & -1 & -1 & -1 & 1 & 0 & 0 & 0 & 1 \\ 1 & -1 & -1 & -1 & -1 & 1 & 0 & 0 & 0 \\ 0 & 1 & -1 & -1 & -1 & -1 & 1 & 0 & 0 \end{bmatrix}.$$

## Appendix C. Proof of proposition 3

Here, we prove that for any strategy in $\mathbf{C}^3_{\text{cs}}$ the payoff is upper bounded by 8. Since $\mathbf{C}^3_{\text{cs}}$ forms a convex set and since the witness $\mathbf{W}_{\text{shift}}$ is linear, the optimal payoff will be achieved for some strategy belonging to $\mathbf{C}^3_{\text{ds}}$. A strategy in $\mathbf{C}^3_{\text{ds}}$ will lead to a $8 \times 64$ Stochastic matrix $\mathcal{S}_d \equiv \{p_d(\mathbf{a}|\mathbf{x},\mathbf{y},\mathbf{z})\}$, where all the entries $p_d(\mathbf{a}|\mathbf{x},\mathbf{y},\mathbf{z})$ are '0' or '1'. For such a strategy the payoff reads as

$$\mathbf{W}_{\text{shift}}\left[\mathcal{S}_d\right] = \sum_{\mathbf{x},\mathbf{y},\mathbf{z},\mathbf{a}} W_{\mathbf{a}|\mathbf{x},\mathbf{y},\mathbf{z}} \times p_d\left(\mathbf{a}|\mathbf{x},\mathbf{y},\mathbf{z}\right) = \sum_{\substack{\mathbf{x},\mathbf{y},\mathbf{z},\mathbf{a} \\ p_d(\mathbf{a}|\mathbf{x},\mathbf{y},\mathbf{z})=1}} W_{\mathbf{a}|\mathbf{x},\mathbf{y},\mathbf{z}} \ . \tag{C1}$$

Instead of considering all the deterministic strategies, we will try to find optimal deterministic decoding strategy for a given deterministic encoding. For a clear exposition we explicitly analyze one such case. Consider the encoding strategy where all senders send the first bit of their respective strings to the receiver, i.e.

$$\mathrm{E}_i = \mathrm{e}^1 := \mathrm{E}^{1\text{st}}_{\text{bit}} : \{00,01\} \mapsto 0, \quad \{10,11\} \mapsto 1; \ \ i \in \{1,2,3\}. \tag{C2}$$

The procedure of finding the optimal decoding strategy for this encoding is described in table 4. It turns out that optimal decoding yields the payoff 8.

**Table 4.** In the first column, $\alpha\beta\gamma$ denotes the message receiver gets from the senders. Second column lists the set of inputs $(\mathbf{x},\mathbf{y},\mathbf{z})$ leading to the corresponding communication $\alpha\beta\gamma$ due to the encoding (C2). The symbols $\chi_{ijk}$ in columns (3-10) denote the payoff obtained for the communication $\alpha\beta\gamma$, given that the receiver decodes $\alpha\beta\gamma \mapsto ijk$. For instance, if the receiver decodes the communication '000' to output '000', i.e. $(\alpha\beta\gamma = 000) \mapsto (ijk = 000)$, then according to the witness $\mathbf{W}_{\text{shift}}$ as defined in equation (9), the payoff for all the possible inputs $\{(00,00,00),(00,00,01),(00,01,00),(00,01,01),(01,00,00),(01,00,01),(01,01,00),(01,01,01)\}$ is $+2$, leading to $\chi_{000} = 8\times 2 = 16$. On the other hand, if the receiver decodes $(\alpha\beta\gamma = 000) \mapsto (ijk = 001)$, then the inputs $\{(00,00,01),(00,01,01),(01,00,01),(01,01,01)\}$ have payoff $-3$ each, and the remaining four possible inputs have payoff $-2$ each. Thus, $\chi_{001} = 4\times(-3)+4\times(-2) = -20$. Rightmost column lists the best possible payoff for the communication $\alpha\beta\gamma$.

| $\alpha\beta\gamma$ | Possible inputs $(\mathbf{x},\mathbf{y},\mathbf{z}) \equiv (x_1x_2, y_1y_2, z_1z_2)$ | $\chi_{000}$ | $\chi_{001}$ | $\chi_{010}$ | $\chi_{011}$ | $\chi_{100}$ | $\chi_{101}$ | $\chi_{110}$ | $\chi_{111}$ | Optimal Decoding | Best Payoff |
|---|---|---|---|---|---|---|---|---|---|---|---|
| 000 | (00,00,00), (00,00,01), (00,01,00), (00,01,01), (01,00,00), (01,00,01), (01,01,00), (01,01,01) | 16 | −20 | −20 | −20 | −20 | −20 | −20 | −16 | 000 | 16 |
| 001 | (00,00,10), (00,00,11), (00,01,10), (00,01,11), (01,00,10), (01,00,11), (01,01,10), (01,01,11) | −24 | −20 | −16 | −4 | −4 | −16 | −20 | −16 | 011/100 | −4 |
| 010 | (00,10,00), (00,10,01), (00,11,00), (00,11,01), (01,10,00), (01,10,01), (01,11,00), (01,11,01) | −24 | −4 | −20 | −16 | −16 | −20 | −4 | −16 | 001/110 | −4 |
| 011 | (00,10,10), (00,10,11), (00,11,10), (00,11,11), (01,10,10), (01,10,11), (01,11,10), (01,11,11) | −16 | −4 | −16 | −20 | −20 | −16 | −4 | −24 | 001/110 | −4 |
| 100 | (10,00,00), (10,00,01), (10,01,00), (10,01,01), (11,00,00), (11,00,01), (11,01,00), (11,01,01) | −24 | −16 | −4 | −20 | −20 | −4 | −16 | −16 | 010/101 | −4 |
| 101 | (10,00,10), (10,00,11), (10,01,10), (10,01,11), (11,00,10), (11,00,11), (11,01,10), (11,01,11) | −16 | −16 | −20 | −4 | −4 | −20 | −16 | −24 | 011/100 | −4 |
| 110 | (10,10,00), (10,10,01), (10,11,00), (10,11,01), (11,10,00), (11,10,01), (11,11,00), (11,11,01) | −16 | −20 | −4 | −16 | −16 | −4 | −20 | −24 | 010/101 | −4 |
| 111 | (10,10,10), (10,10,11), (10,11,10), (10,11,11), (11,10,10), (11,10,11), (11,11,10), (11,11,11) | −16 | −20 | −20 | −20 | −20 | −20 | −20 | 16 | 111 | 16 |
| | **Total Payoff (TP)** | | | | | | | | | | **8** |

Up-to the freedom of relabeling, each sender can chose their deterministic encoding from the following set of eight deterministic encodings:

$$\mathcal{E} \equiv \left\{ \begin{array}{llll} \mathrm{e}^0 := \mathrm{E}_{\text{const}} : \{00,01,10,11\} \mapsto 0,\ \{\} \mapsto 1; & \mathrm{e}^1 := \mathrm{E}^{\text{1st}}_{\text{bit}} : \{00,01\} \mapsto 0, & \{10,11\} \mapsto 1; \\ \mathrm{e}^2 := \mathrm{E}^{\text{2nd}}_{\text{bit}} : \{00,10\} \mapsto 0, & \{01,11\} \mapsto 1; & \mathrm{e}^3 := \mathrm{E}_{\text{par}} : \{00,11\} \mapsto 0, & \{01,10\} \mapsto 1; \\ \mathrm{e}^4 := \mathrm{E}^{1|3}_{00} : \{00\} \mapsto 0, & \{01,10,11\} \mapsto 1; & \mathrm{e}^5 := \mathrm{E}^{1|3}_{01} : \{01\} \mapsto 0, & \{00,10,11\} \mapsto 1; \\ \mathrm{e}^6 := \mathrm{E}^{1|3}_{10} : \{10\} \mapsto 0, & \{00,01,11\} \mapsto 1; & \mathrm{e}^7 := \mathrm{E}^{1|3}_{11} : \{11\} \mapsto 0, & \{00,01,10\} \mapsto 1; \end{array} \right\}. \tag{C3}$$

While in table 4 we analyze the case where three senders follow the encoding $\left(\mathrm{e}^1,\mathrm{e}^1,\mathrm{e}^1\right)$, similar analysis can be accomplished efficiently for $8^3$ different encoding triples $(\mathrm{e}^p,\mathrm{e}^q,\mathrm{e}^r) \in \mathcal{E}\times\mathcal{E}\times\mathcal{E}$, where $p,q,r \in \{0,1,\cdots,7\}$. In table 5 we list the optimal total payoff (TP) for all these encodings, which in turn proves the claim of proposition 3.

**Table 5.** Optimal total payoff (TP) are listed for all the $8^3$ encoding strategies $(e^i, e^j, e^k) \equiv (i, j, k)$, for $i, j, k \in \{0, 1, \cdots, 7\}$. The optimal classical payoff turns out to be **8**, achieved for the encoding $(e^1, e^1, e^1) \equiv (1, 1, 1)$.

| Encoding | | | TP |
|---|---|---|---|
| $e^i$ | $e^j$ | $e^k$ | |
| 0 | 0 | 0, 3 | −120 |
| | 3 | 0, 3 | |
| 3 | 0 | 0, 3 | |
| | 3 | 0, 3 | |
| 0 | 0 | 4, 5, 6, 7 | −108 |
| | 3 | 4, 5, 6, 7 | |
| | 4 | 0, 3 | |
| | 5 | 0, 3 | |
| | 6 | 0, 3 | |
| | 7 | 0, 3 | |
| 3 | 0 | 4, 5, 6, 7 | |
| | 3 | 4, 5, 6, 7 | |
| | 4 | 0, 3 | |
| | 5 | 0, 3 | |
| | 6 | 0, 3 | |
| | 7 | 0, 3 | |
| 4 | 0 | 0, 3 | |
| | 3 | 0, 3 | |
| 5 | 0 | 0, 3 | |
| | 3 | 0, 3 | |
| 6 | 0 | 0, 3 | |
| | 3 | 0, 3 | |
| 7 | 0 | 0, 3 | |
| | 3 | 0, 3 | |
| 0 | 0 | 1, 2 | −96 |
| | 1 | 0, 3 | |
| | 2 | 0, 2, 3 | |
| | 3 | 1, 2 | |
| 1 | 0 | 0, 3 | |
| | 3 | 0, 3 | |
| 2 | 0 | 0, 2, 3 | |
| | 2 | 0, 2, 3 | |
| | 3 | 0, 2, 3 | |
| 3 | 0 | 1, 2 | |
| | 1 | 0, 3 | |
| | 2 | 0, 2, 3 | |
| | 3 | 1, 2 | |
| 0 | 2 | 4, 5 | −92 |
| | 6 | 2 | |
| | 7 | 2 | |
| 2 | 0 | 6, 7 | |
| | 3 | 6, 7 | |
| | 4 | 0, 3 | |
| | 5 | 0, 3 | |
| 3 | 2 | 4, 5 | |
| | 6 | 2 | |
| | 7 | 2 | |
| 4 | 0 | 2 | |
| | 3 | 2 | |
| 5 | 0 | 2 | |
| | 3 | 2 | |
| 6 | 2 | 0, 3 | |
| 7 | 2 | 0, 3 | |
| 0 | 4 | 4, 5, 6, 7 | −86 |
| | 5 | 4, 5, 6, 7 | |
| | 6 | 4, 5, 6, 7 | |
| | 7 | 4, 5, 6, 7 | |
| 3 | 4 | 4, 5, 6, 7 | |
| | 5 | 4, 5, 6, 7 | |
| | 6 | 4, 5, 6, 7 | |
| | 7 | 4, 5, 6, 7 | |
| ⇓ | | | |

| | | | |
|---|---|---|---|
| 4 | 0 | 4, 5, 6, 7 | −86 |
| | 3 | 4, 5, 6, 7 | |
| | 4 | 0, 3 | |
| | 5 | 0, 3 | |
| | 6 | 0, 3 | |
| | 7 | 0, 3 | |
| 5 | 0 | 4, 5, 6, 7 | |
| | 3 | 4, 5, 6, 7 | |
| | 4 | 0, 3 | |
| | 5 | 0, 3 | |
| | 6 | 0, 3 | |
| | 7 | 0, 3 | |
| 6 | 0 | 4, 5, 6, 7 | |
| | 3 | 4, 5, 6, 7 | |
| | 4 | 0, 3 | |
| | 5 | 0, 3 | |
| | 6 | 0, 3 | |
| | 7 | 0, 3 | |
| 7 | 0 | 4, 5, 6, 7 | |
| | 3 | 4, 5, 6, 7 | |
| | 4 | 0, 3 | |
| | 5 | 0, 3 | |
| | 6 | 0, 3 | |
| | 7 | 0, 3 | |
| 0 | 2 | 6, 7 | −80 |
| | 4 | 2 | |
| | 5 | 2 | |
| 2 | 0 | 4, 5 | |
| | 3 | 4, 5 | |
| | 6 | 0, 3 | |
| | 7 | 0, 3 | |
| 3 | 2 | 6, 7 | |
| | 4 | 2 | |
| | 5 | 2 | |
| 4 | 2 | 0, 3 | |
| 5 | 2 | 0, 3 | |
| 6 | 0 | 2 | |
| | 3 | 2 | |
| 7 | 0 | 2 | |
| | 3 | 2 | |
| 2 | 4 | 6, 7 | −76 |
| | 5 | 6, 7 | |
| 4 | 6 | 2 | |
| | 7 | 2 | |
| 5 | 6 | 2 | |
| | 7 | 2 | |
| 6 | 2 | 4, 5 | |
| 7 | 2 | 4, 5 | |
| 2 | 4 | 4, 5 | −68 |
| | 5 | 4, 5 | |
| | 6 | 6, 7 | |
| | 7 | 6, 7 | |
| 4 | 2 | 4, 5 | |
| | 4 | 2 | |
| | 5 | 2 | |
| 5 | 2 | 4, 5 | |
| | 4 | 2 | |
| | 5 | 2 | |
| 6 | 2 | 6, 7 | |
| | 6 | 2 | |
| | 7 | 2 | |
| ⇓ | | | |

| | | | |
|---|---|---|---|
| 7 | 2 | 6, 7 | −68 |
| | 6 | 2 | |
| | 7 | 2 | |
| 0 | 1 | 2, 4, 5, 6, 7 | −64 |
| | 2 | 1 | |
| | 4 | 1 | |
| | 5 | 1 | |
| | 6 | 1 | |
| | 7 | 1 | |
| 1 | 0 | 2, 4, 5, 6, 7 | |
| | 2 | 0, 3 | |
| | 3 | 2, 4, 5, 6, 7 | |
| | 4 | 0, 3 | |
| | 5 | 0, 3 | |
| | 6 | 0, 3 | |
| | 7 | 0, 3 | |
| 2 | 0 | 1 | |
| | 1 | 0, 3 | |
| | 2 | 4, 5, 6, 7 | |
| | 3 | 1 | |
| | 4 | 2 | |
| | 5 | 2 | |
| | 6 | 2 | |
| | 7 | 2 | |
| 3 | 1 | 2, 4, 5, 6, 7 | |
| | 2 | 1 | |
| | 4 | 1 | |
| | 5 | 1 | |
| | 6 | 1 | |
| | 7 | 1 | |
| 4 | 0 | 1 | |
| | 1 | 0, 3 | |
| | 2 | 2 | |
| | 3 | 1 | |
| 5 | 0 | 1 | |
| | 1 | 0, 3 | |
| | 2 | 2 | |
| | 3 | 1 | |
| 6 | 0 | 1 | |
| | 1 | 0, 3 | |
| | 2 | 2 | |
| | 3 | 1 | |
| 7 | 0 | 1 | |
| | 1 | 0, 3 | |
| | 2 | 2 | |
| | 3 | 1 | |
| 2 | 6 | 4, 5 | −54 |
| | 7 | 4, 5 | |
| 4 | 2 | 6, 7 | |
| 5 | 2 | 6, 7 | |
| 6 | 4 | 2 | |
| | 5 | 2 | |
| 7 | 4 | 2 | |
| | 5 | 2 | |
| 0 | 1 | 1 | −48 |
| 1 | 0 | 1 | |
| | 1 | 0, 3 | |
| | 3 | 1 | |
| 3 | 1 | 1 | |
| 4 | 4 | 4, 5, 6, 7 | −47 |
| | 5 | 4, 5, 6, 7 | |
| ⇓ | | | |

| | | | |
|---|---|---|---|
| 4 | 6 | 4, 5, 6, 7 | −47 |
| | 7 | 4, 5, 6, 7 | |
| 5 | 4 | 4, 5, 6, 7 | |
| | 5 | 4, 5, 6, 7 | |
| | 6 | 4, 5, 6, 7 | |
| | 7 | 4, 5, 6, 7 | |
| 6 | 4 | 4, 5, 6, 7 | |
| | 5 | 4, 5, 6, 7 | |
| | 6 | 4, 5, 6, 7 | |
| | 7 | 4, 5, 6, 7 | |
| 7 | 4 | 4, 5, 6, 7 | |
| | 5 | 4, 5, 6, 7 | |
| | 6 | 4, 5, 6, 7 | |
| | 7 | 4, 5, 6, 7 | |
| 1 | 2 | 4, 5 | −44 |
| | 6 | 2 | |
| | 7 | 2 | |
| 2 | 1 | 6, 7 | |
| | 4 | 1 | |
| | 5 | 1 | |
| 4 | 1 | 2 | |
| 5 | 1 | 2 | |
| 6 | 2 | 1 | |
| 7 | 2 | 1 | |
| 1 | 6 | 4, 5 | −40 |
| | 7 | 4, 5 | |
| 4 | 1 | 6, 7 | |
| 5 | 1 | 6, 7 | |
| 6 | 4 | 1 | |
| | 5 | 1 | |
| 7 | 4 | 1 | |
| | 5 | 1 | |
| 1 | 2 | 2 | −32 |
| 2 | 1 | 2 | |
| | 2 | 1 | |
| 1 | 2 | 6, 7 | −28 |
| | 4 | 2 | |
| | 5 | 2 | |
| 2 | 1 | 4, 5 | |
| | 6 | 1 | |
| | 7 | 1 | |
| 4 | 2 | 1 | |
| 5 | 2 | 1 | |
| 6 | 1 | 2 | |
| 7 | 1 | 2 | |
| 1 | 4 | 4, 5 | −26 |
| | 5 | 4, 5 | |
| | 6 | 6, 7 | |
| | 7 | 6, 7 | |
| 4 | 1 | 4, 5 | |
| | 4 | 1 | |
| | 5 | 1 | |
| 5 | 1 | 4, 5 | |
| | 4 | 1 | |
| | 5 | 1 | |
| 6 | 1 | 6, 7 | |
| | 6 | 1 | |
| | 7 | 1 | |
| 7 | 1 | 6, 7 | |
| | 6 | 1 | |
| | 7 | 1 | |
| ⇓ | | | |

| | | | |
|---|---|---|---|
| 1 | 4 | 6, 7 | −18 |
| | 5 | 6, 7 | |
| 4 | 6 | 1 | |
| | 7 | 1 | |
| 5 | 6 | 1 | |
| | 7 | 1 | |
| 6 | 1 | 4, 5 | |
| 7 | 1 | 4, 5 | |
| 1 | 1 | 2, 4, 5, 6, 7 | −8 |
| | 2 | 1 | |
| | 4 | 1 | |
| | 5 | 1 | |
| | 6 | 1 | |
| | 7 | 1 | |
| 2 | 1 | 1 | |
| 4 | 1 | 1 | |
| 5 | 1 | 1 | |
| 6 | 1 | 1 | |
| 7 | 1 | 1 | |
| **1** | **1** | **1** | **8** |
| ⇓ | | | |

## ORCID iDs

Ananya Chakraborty https://orcid.org/0009-0009-8075-4497
Sahil Gopalkrishna Naik https://orcid.org/0000-0002-9645-0609
Edwin Peter Lobo https://orcid.org/0000-0001-5806-0389
Ram Krishna Patra https://orcid.org/0000-0001-9397-0476
Samrat Sen https://orcid.org/0000-0002-0998-286X
Mir Alimuddin https://orcid.org/0000-0002-5243-085X
Amit Mukherjee https://orcid.org/0000-0001-8330-8198
Manik Banik https://orcid.org/0000-0001-8036-790X

## References

[1] Shannon C E 1948 A mathematical theory of communication *Bell Syst. Tech. J.* **27** 379
[2] Wilde M M 2011 From classical to quantum Shannon theory (arXiv:1106.1445 [quant-ph])
[3] Nielsen M A and Chuang I L 2010 *Quantum Computation and Quantum Information* 10th Anniversary edn (Cambridge University Press)
[4] Bennett C H and Wiesner S J 1992 Communication via one- and two-particle operators on Einstein-Podolsky-Rosen states *Phys. Rev. Lett.* **69** 2881
[5] Adami C and Cerf N J 1997 von Neumann capacity of noisy quantum channels *Phys. Rev.* A **56** 3470
[6] Bennett C H, Shor P W, Smolin J A and Thapliyal A V 1999 Entanglement-assisted classical capacity of noisy quantum channels *Phys. Rev. Lett.* **83** 3081
[7] Bennett C H, Shor P W, Smolin J A and Thapliyal A V 2002 Entanglement-assisted capacity of a quantum channel and the reverse Shannon theorem *IEEE Trans. Inf. Theory* **48** 2637
[8] Holevo A S 1973 Bounds for the quantity of information transmitted by a quantum communication channel *Probl. Inf. Transm.* **9** 177
[9] Frenkel P E and Weiner M 2015 Classical information storage in an n-level quantum system *Commun. Math. Phys.* **340** 563
[10] Dall'Arno M, Brandsen S, Tosini A, Buscemi F, Vedral V Principle N-H 2017 *Phys. Rev. Lett.* **119** 020401
[11] Naik S G, Lobo E P, Sen S, Patra R K, Alimuddin M, Guha T, Bhattacharya S S and Banik M 2022 Composition of multipartite quantum systems: perspective from timelike paradigm *Phys. Rev. Lett.* **128** 140401
[12] Sen S, Lobo E P, Patra R K, Naik S G, Bhowmik A D, Alimuddin M and Banik M 2022 Timelike correlations and quantum tensor product structure *Phys. Rev.* A **106** 062406
[13] Patra R K, Naik S G, Lobo E P, Sen S, Sidhardh G L, Alimuddin M and Banik M 2023 Principle of information causality rationalizes quantum composition *Phys. Rev. Lett.* **130** 110202
[14] Gamel A E and Kim Y-H 2011 *Network Information Theory* (Cambridge University Press) (https://doi.org/10.1017/CBO9781139030687)
[15] Ahlswede R 1971 Multi-way communication channels *2nd Int. Symp. on Information Theory: Tsahkadsor (Armenia, USSR)* pp 23–52
[16] Liao H 1972 Multiple access channels *PhD Thesis* Department of Electrical Engineering, University of Hawaii
[17] Biglieri E and Györfi L (eds) 2007 *Multiple Access Channels [Nato Security Through Science Series, D* vol 10
[18] Yard J, Hayden P and Devetak I 2008 Capacity theorems for quantum multiple-access channels: classical-quantum and quantum-quantum capacity regions *IEEE Trans. Inf. Theor.* **54** 3091
[19] Pusey M F, Barrett J and Rudolph T 2012 On the reality of the quantum state *Nat. Phys.* **8** 475
[20] Bennett C H, DiVincenzo D P, Fuchs C A, Mor T, Rains E, Shor P W, Smolin J A and Wootters W K 1999 Quantum nonlocality without entanglement *Phys. Rev.* A **59** 1070
[21] Patra R K, Naik S G, Lobo E P, Sen S, Guha T, Bhattacharya S S, Alimuddin M and Banik M 2024 Classical analogue of quantum superdense coding and communication advantage of a single quantum system *Quantum* B **8** 1315
[22] Ding C, Lobo E P, Alimuddin M, Xu X, Zhang S, Banik M, Bao W and Huang H 2024 Quantum advantage: a single qubit's experimental edge in classical data storage *Phys. Rev. Lett.* **133** 200201
[23] Heinosaari T, Kerppo O, Leppäjärvi L and Plávala M 2024 Simple information-processing tasks with unbounded quantum advantage *Phys. Rev.* A **109** 032627
[24] Boyd S and Vandenberghe L 2004 *Convex Optimization* (Cambridge University Press)
[25] Buhrman H, Cleve R, Massar S, de Wolf R 2010 Nonlocality and communication complexity *Rev. Mod. Phys.* **82** 665
[26] Wiesner S 1983 Conjugate coding *SIGACT News* **15** 78
[27] Ambainis A Nayak A Ta-Shma A and Vazirani U 2002 Dense quantum coding and quantum finite automata *J. ACM* **49** 496
[28] Ambainis A, Banik M, Chaturvedi A, Kravchenko D and Rai A 2019 Parity oblivious d-level random access codes and class of noncontextuality inequalities *Quantum Inf. Process.* **18** 111
[29] Bhattacharya S S, Saha S, Guha T and Banik M 2020 Nonlocality without entanglement: Quantum theory and beyond *Phys. Rev. Res.* **2** 012068(R)
[30] Niset J and Cerf N J 2006 Multipartite nonlocality without entanglement in many dimensions *Phys. Rev.* A **74** 052103
[31] Bennett C H and Shor P W 1998 Quantum information theory *IEEE Trans. Inf. Theory* **44** 2724
[32] Fuchs C A 1997 Nonorthogonal quantum states maximize classical information capacity *Phys. Rev. Lett.* **79** 1162
[33] Holevo A S 1998 The capacity of quantum channel with general signal states *IEEE Trans. Inf. Theory* **44** 269
[34] Hastings M 2009 Superadditivity of communication capacity using entangled inputs *Nat. Phys.* **5** 255
[35] King C and Ruskai M B 2001 Capacity of quantum channels using product measurements *J. Math. Phys.* **42** 87
[36] Lo H-K 2000 Classical-communication cost in distributed quantum-information processing: a generalization of quantum-communication complexity *Phys. Rev.* A **62** 012313
[37] Pati A K 2000 Minimum classical bit for remote preparation and measurement of a qubit *Phys. Rev.* A **63** 014302
[38] Bennett C H, DiVincenzo D P, Shor P W, Smolin J A, Terhal B M and Wootters W K 2001 Remote state preparation *Phys. Rev. Lett.* **87** 077902

[39] Quek Y and Shor P W 2017 Quantum and superquantum enhancements to two-sender, two-receiver channels *Phys. Rev.* A **95** 052329
[40] Leditzky F, Alhejji M A, Levin J and Smith G 2020 Playing games with multiple access channels *Nat. Commun.* **11** 1497
[41] Yun J, Rai A and Bae J 2020 Nonlocal network coding in interference channels *Phys. Rev. Lett.* **125** 150502
[42] Harrigan N and Spekkens R W 2010 Einstein, incompleteness and the epistemic view of quantum states *Found. Phys.* **40** 125
[43] Renou M-O, Bäumer E, Boreiri S, Brunner N Gisin N and Beigi S 2019 Genuine quantum nonlocality in the triangle network *Phys. Rev. Lett.* **123** 140401
[44] Tavakoli A Pozas-Kerstjens A, Luo M-X and Renou M-O 2022 Bell nonlocality in networks *Rep. Prog. Phys.* **85** 056001
[45] Vértesi T and Navascués M 2011 Certifying entangled measurements in known Hilbert spaces *Phys. Rev.* A **83** 062112
[46] Bennet A, Vértesi T, Saunders D J, Brunner N and Pryde G J 2014 Experimental semi-device-independent certification of entangled measurements *Phys. Rev. Lett.* **113** 080405
[47] Šupić I and Brunner N 2023 Self-testing nonlocality without entanglement *Phys. Rev.* A **107** 062220
[48] Halder S, Banik M, Agrawal S and Bandyopadhyay S 2019 Strong quantum nonlocality without entanglement *Phys. Rev. Lett.* **122** 040403
[49] Rout S, Maity A G, Mukherjee A, Halder S and Banik M 2019 Genuinely nonlocal product bases: classification and entanglement-assisted discrimination *Phys. Rev.* A **100** 032321
[50] Ghosh S B, Gupta T, Ardra A V, Bhowmik A D, Saha S, Guha T and Mukherjee A 2022 Activating strong nonlocality from local sets: An elimination paradigm *Phys. Rev.* A **106** L010202
[51] Cirac J I, Ekert A K and Macchiavello C 1999 Optimal purification of single qubits *Phys. Rev. Lett.* **82** 4344
[52] Ricci M, De Martini F, Cerf N J, Filip R, Fiurášek J and Macchiavello C 2004 Experimental purification of single qubits *Phys. Rev. Lett.* **93** 170501
[53] Okamoto R, O'Brien J L, Hofmann H F, Nagata T, Sasaki K and Takeuchi S 2009 An Entanglement Filter *Science* **323** 483
[54] Zhou X-Q, Ralph T C, Kalasuwan P, Zhang M, Peruzzo A, Lanyon B P and O'Brien J L 2011 Adding control to arbitrary unknown quantum operations *Nat. Commun.* **2** 413
[55] Watson T F *et al* 2018 A programmable two-qubit quantum processor in silicon *Nature* **555** 633
[56] Lu Y, Zhang S, Zhang K, Chen W, Shen Y, Zhang J, Zhang J-N and Kim K 2019 Global entangling gates on arbitrary ion qubits *Nature* **572** 363
[57] Stas P-J *et al* 2022 Robust multi-qubit quantum network node with integrated error detection *Science* **378** 557